

Strong observational constraints on Advection-Dominated Accretion in the cores of elliptical galaxies

T. Di Matteo¹, A. C. Fabian¹, M. J. Rees¹, C. L. Carilli² and R. J. Ivison³

¹Institute of Astronomy, Madingley Road, Cambridge, CB3 0HA

²NRAO, P.O. Box O, Socorro, NM, 87801, USA

³Institute for Astronomy, Dept. of Physics & Astronomy, University of Edinburgh, Blackford Hill, Edinburgh EH9 3HJ

23 March 2018

ABSTRACT

The growing evidence for supermassive black holes in the centres of relatively nearby galaxies has brought into sharper focus the question of why elliptical galaxies, rich in hot gas, do not possess quasar-like luminosities. Recent studies suggest that the presence of advection-dominated accretion flows (ADAFs) with their associated low radiative efficiency, might provide a very promising explanation for the observed quiescence of these systems. Although ADAF models have been applied to a number of low-luminosity systems compelling observational evidence for their existence is still required. Here, we examine new high-frequency radio observations of the three giant, low-luminosity elliptical galaxies NGC 4649, NGC 4472 and NGC 4636 obtained using the Very Large Array (VLA) and the sub-millimetre common-user bolometer array (SCUBA) on the James Clerk Maxwell Telescope (JCMT). At these frequencies the predictions are very precise and an ADAF is unequivocally characterised by a slowly rising spectrum with a sharp spectral cut-off produced by thermal synchrotron radiation. Although X-ray analysis of these galaxy cores provides very strong clues for their extreme quiescence (and makes the case of advective-accretion plausible) the new radio limits disagree severely with the canonical ADAF predictions which significantly overestimate the observed flux. While the present observations do not rule out the presence of an ADAF in the systems considered here, they do place strong constraints on the model. If the accretion in these objects occurs in an advection-dominated mode then our radio limits imply that the emission from their central regions must be suppressed. We examine the possibility that the magnetic field in the flow is extremely low or that synchrotron emission is free-free absorbed by cold material in the accretion flow. We also discuss whether slow non-radiating accretion flows may drive winds/outflows to remove energy, angular momentum and mass so that the central densities, pressure and emissivities are much smaller than in a standard ADAF.

Key words: galaxies: individual: NGC 4649 – NGC 4472 – NGC 4636, galaxies: active, accretion, accretion discs

1 INTRODUCTION

Clear evidence for supermassive black holes comes from studies of nearby galaxies. The centres of most of these galaxies display little or no activity, but most seem to harbour massive black holes probably remnants of an earlier quasar phase (Kormendy and Richstone 1995, Tremaine 1997 for recent reviews). It is a puzzle why the massive black holes in the nearby galaxies do not show quasar-like activity. The problem becomes particularly relevant for the case of nearby giant elliptical galaxies where it is implausible to postulate that the black holes are ‘starved’ of fuel to power the accretion process. X-ray studies for such giant ellipticals

reveal the presence of an extensive hot gas pervading their centres (as well as the surrounding cluster). If there were a huge black hole then some of this gas would inevitably be accreting into it, at a rate which can be estimated from the Bondi (1952) formula (a lower limit). This accretion would give rise to far more activity than is observed if the radiative efficiency were as high as 10 per cent as generally postulated in standard accretion theory (Fabian & Canizares 1988).

Motivated by this problem Fabian & Rees (1995) have recently suggested that the final stages of accretion in such objects occurs through an advection-dominated accretion flow (ADAF; Narayan & Yi 1995, Abramovicz et al. 1995). Within the context of such an accretion mode, the quies-

cence of these nuclei is not surprising. For low accretion rates, the expected luminosity scales as \dot{M}^2 rather than \dot{M} : when the accretion occurs at a low rate, and the viscosity is high enough to ensure that the gas accretes quickly (and densities are low), the radiative efficiency is low. The gas inflates into a thick torus where the kinetic temperature of the ions is close to the virial temperature. Only a small fraction of the gravitational energy is radiated; most is swallowed into the black hole.

The relevance of this accretion solution in ellipticals has been illustrated by its application to the giant elliptical galaxy M87 (NGC 4486). This has a quiescent active nucleus the luminosity of which does not exceed $10^{42} \text{ erg s}^{-1}$ with a nuclear black hole mass $M \approx 3 \times 10^9 M_\odot$ (Ford et al. 1994; Harms et al. 1994, Macchetto et al. 1997). The radio and X-ray emission in M87 is fully consistent with accretion at the expected rate only if it involves an ADAF (Reynolds et al. 1996). Furthermore, it has been shown that if elliptical galaxies like M60 (NGC 4649, Di Matteo & Fabian 1997) or NGC 4472, NGC 4636 (Mahadevan 1997) have advection-dominated nuclei then the upper limit on their nuclear mass black hole can be of the order of $M \sim 10^9 M_\odot$, thereby allowing supermassive black holes in these systems.

Although accretion of hot gas in an elliptical galaxy may create the ideal circumstances for an ADAF to operate, stronger observational evidence needs to be obtained. In this paper we examine how ADAF models of nuclei in ellipticals can be constrained with further high frequency radio and submillimeter data.

1.1 Testing the ADAF paradigm for elliptical galaxies

In an ADAF, the majority of the observable emission is in the radio and X-ray bands. In the radio band the emission results from cyclo-synchrotron emission due to the strong magnetic field in the inner parts of the accretion flow. The X-ray emission is due either to bremsstrahlung or inverse Compton scattering. On the observational side, therefore, the cleanest way of determining the presence of an ADAF is to examine the correlation between radio and X-ray emissions. The spectral predictions of the ADAF model are quite precise in these wavebands and the expected correlation tight. Weak central radio sources are observed in the centres of many otherwise quiescent ellipticals (Sadler et al. 1989). If these galaxies all harbour massive black holes, this radio emission could similarly be attributed to the synchrotron radiation in an inefficient accretion mode (i.e. an ADAF).

The self-absorbed synchrotron spectrum in an ADAF slowly rises with frequency in the radio band, up to some critical turnover frequency, typically in high radio to sub-mm frequencies, above which it should abruptly drop. A large spectral break there is crucially indicative of thermal self-absorbed synchrotron emission. Observations of a slowly-rising spectrum which sharply cuts off in the sub-mm band, would provide the cleanest evidence that such an accretion mode is taking place in nearby galaxies.

Here, we examine the high-frequency Very Large Array (VLA) and Submillimeter Common User Bolometer Array (SCUBA) data for three giant ellipticals in the Virgo cluster NGC 4649, NGC 4636, and NGC 4472 where the spectral turnover should be seen. Slee et al. (1994) show

Table 1. Black hole masses (Magorrian et al. 1998) and predicted luminosities

Object	Black Hole ($10^9 M_\odot$)	$L_{\text{predicted}}$ ($10^{44} \text{ erg s}^{-1}$)
NGC 4649	3.9	5.1
NGC 4472	2.6	2.3
NGC 4636	0.3	0.03

that the size of most of the radio cores in elliptical galaxies is on the parsec scale or less which would imply that they are powered by an engine similar to that in more luminous radio galaxies. It is interesting to note that these authors find that the cores of ellipticals usually have flat or rising spectra. The motivation for the choice of these galaxies is two-fold. On one hand, the radio data already existing (Fabiano et al. 1988) for both NGC 4649 and NGC 4636 imply a flat/slowly rising radio spectral component and therefore a tentative agreement with the ADAF predictions in the intermediate-frequency radio band. In particular the radio spectrum of NGC 4649 was shown to closely resemble that expected from the self-absorbed synchrotron radiation (Di Matteo & Fabian 1997).

On the other hand, as discussed above, these giant elliptical galaxies seem to be the strongest candidates for illustrating the possibility of explaining quiescent accretion via ADAFs. Recent *Hubble Space Telescope (HST)* observations (Magorrian et al. 1998) have now provided high resolution dynamical models for these and many other nearby galaxies and a determination of nuclear black hole masses of the order of $10^8 - 10^9 M_\odot$ (see Table 1).

A deprojection analysis of data from the *ROSAT* High Resolution Imager (HRI) shows that the hot interstellar medium (ISM) in NGC 4649, 4472 and 4636 has a central density $n \approx 0.1 \text{ cm}^{-3}$ for a sound speed $c_s \sim 300 \text{ km s}^{-1}$. The resulting Bondi accretion rate onto a central black hole of $10^9 M_\odot$ is then

$$\dot{M}_{\text{Bondi}} \sim 10^{-2} \left(\frac{M}{10^9 M_\odot} \right)^2 \left(\frac{n_\infty}{0.1} \right) \left(\frac{300}{c_\infty} \right)^3 M_\odot \text{ yr}^{-1}. \quad (1)$$

For the black hole masses predicted for these galaxies (Table 1; Magorrian et al. 1998) the Bondi rate, for a radiative efficiency of $\eta = 0.1$ (as assumed for standard accretion) predicts a luminosity of the order of $L_{\text{predicted}}$ exceeding $10^{44} \text{ erg s}^{-1}$ for two of them (see Table 1). Observationally, the nuclei of these giant ellipticals are orders of magnitude less active (see Fig. 5 and 6). The observed luminosity of their cores does not exceed $10^{40} \text{ erg s}^{-1}$ over all energies. In this paper we test the ADAF paradigm for elliptical galaxies by analysing high frequency radio and sub-mm data together with X-ray *ROSAT* HRI observations. In Section 2, we show our VLA and SCUBA data, present upper limits for the X-ray flux from the core, and summarize some other relevant data from the literature on the full-band spectrum of the cores of NGC 4649, 4636 and 4472. Section 3 describes some details of our ADAF model spectrum calculation. In Section 4, we compare the model spectrum with the data and find very strong new constraints for the ADAF mod-

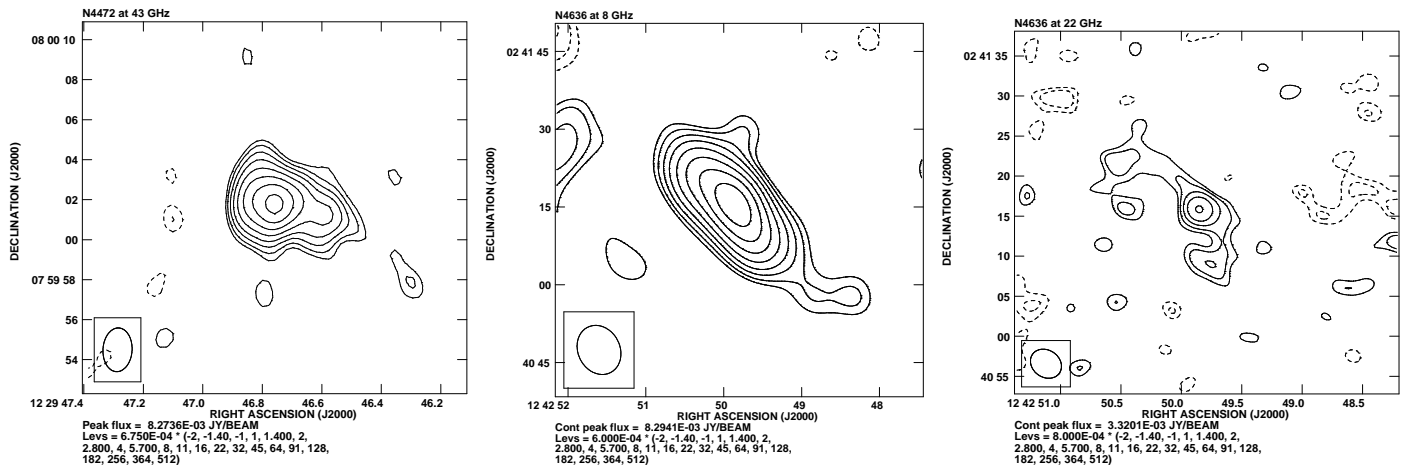


Figure 1. VLA high resolution radio images for NGC 4472 at 43 GHz and NGC 4636 at 8 and 22 GHz. The FWHM of the restoring Gaussian beam is shown in the box in lower left corner. These are the two extended sources in the sample.

Table 2. SCUBA observations.

Object	Wavelength mm	Flux mJy
NGC 4649	2.0	1.8 ± 1.7
NGC 4472	2.0	9.6 ± 2.4
	1.35	4.5 ± 1.1
	0.85	3.0 ± 1.3
NGC 4636	–	

els. Section 5, discusses some important implications of our results.

As mentioned above, demonstrating that accretion via ADAFs is operating in the nearby universe would be an important step in understanding the demise of quasars.

2 THE SPECTRUM OF THE CORE EMISSION

In order to examine the nature of the accretion flow in elliptical galaxies, we have compiled the best observational limits on the full band spectrum of the core emission. Our aim is to obtain good observational limits on the core flux over a wide range of frequencies rather than to compile a comprehensive list of all previous observations. Some contribution from the weak jets and in particular from the underlying galaxy are unavoidable and so the derived spectrum should be considered an upper limit to that of the accretion flow at the elliptical galaxies cores.

In the next two sections we present our new high frequency radio and sub-mm (VLA and SCUBA respectively) observations and ROSAT HRI upper limits to the X-ray emission. High radio frequency and sub-mm observations together with X-ray measurements are crucial for constraining the case of ADAFs in elliptical galaxy cores. The data for NGC 4649, NGC 4472 and NGC 4636 are summarized in Table 4, 5 and 6 respectively.

2.1 The radio data

Radio continuum surveys of elliptical and S0 galaxies have shown that the sources in radio-quiet galaxies tend to be compact with relatively flat or slowly rising radio spectra (with typical spectral index of 0.3–0.4), suggesting that the radio emission from ellipticals are in general of nuclear origin (Slee et al. 1994; Wrobel 1991) and might be powered by engines similar to those in more luminous radio galaxies.

Very Large Array (VLA) imaging by Stanger & Warwick (1986) and Wrobel & Heeshen (1991; at $\nu = 5$ GHz) has shown that the nuclear radio sources in NGC 4649, NGC 4472 and NGC 4636 are extended with a compact ($\lesssim 4$ arcsec), core component. The extended structure defines radio lobes powered by weak jets with linear dimensions ~ 2 kpc. The relatively flat/slowly-rising spectral nature of the high-frequency emission from NGC 4636 and NGC 4649, which is well defined by the data of Fabbiano et al. (1987) (see Table 4 and 6), motivated the selection of these galaxies for further higher frequency observations. NGC 4472 also follows the same general trend (Wrobel & Heeshen 1991)

2.2 VLA and SCUBA Observations

Measurements of all three galaxies were obtained with the Very Large Array (VLA) at 8.4, 22 and 43 GHz during December 1997. The resulting data are shown in Table 3. NGC 4472 and 4636 are extended sources and their high resolution radio images are shown in Fig. 1. In order to obtain the best limits on the core flux for the extended sources, the flux densities were derived from images convolved to the resolution of the 8 GHz image at all frequencies (fifth column in Table 3). The full-width-at-half-maximum (FWHM) of Gaussian restoring beam at 8 GHz ($\delta = -8$ deg) was 9×8 arcsec². The flux scale was set using 3C 286.

On January 30, 1998, NGC 4649 and NGC 4472 were also observed in the submillimeter band using the new SCUBA bolometer camera (Holland et al. 1998; Robson et al. 1998) on the JCMT. Data were obtained at 450, 850, 1350 and 2000 μm during a good, stable night. The photometry scans were interspersed with checks on the accuracy of the

Table 3. VLA data

Galaxy	Frequency	RMS	Total	Peak	Peak	notes
	ν (GHz)	mJy	F_ν (mJy)	F_ν (mJy)	at 8GHz resolution F_ν (mJy)	
NGC 4649	8.4	0.10	18.1 ± 0.9	17.6 ± 0.9	–	point source
	22	0.30	23.5 ± 1.4	21.9 ± 1.3	–	
	43	0.27	12.9 ± 1.3	12.7 ± 1.3	–	
NGC 4472	8.4	0.30	49.0 ± 2.5	44.0 ± 2.2	44.0 ± 2.2	extended source
	22	0.32	34.0 ± 2.0	23.9 ± 1.4	31.9 ± 1.9	
	43	0.22	23.5 ± 2.4	8.3 ± 0.8	20.7 ± 1.7	
NGC 4636	8.4	0.33	18.1 ± 0.9	8.3 ± 0.4	8.3 ± 0.4	extended source
	22	0.48	13.5 ± 1.4	3.3 ± 0.5	5.6 ± 1.2	
	43	0.22	–	0.6 ± 0.2	< 1.8	

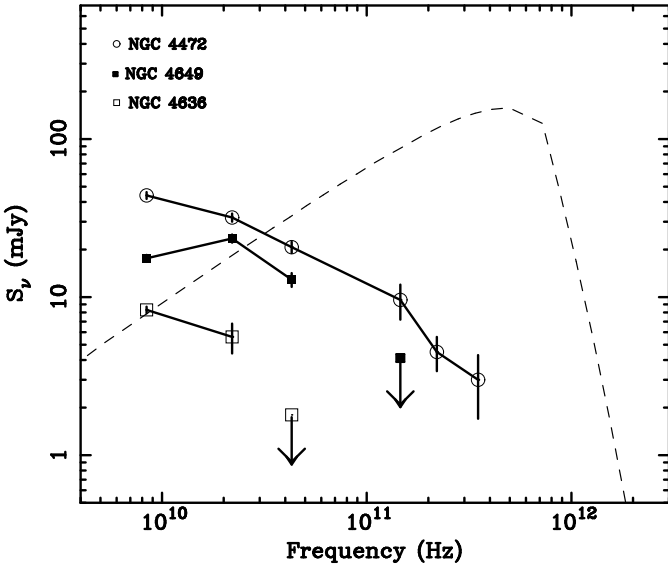


Figure 2. The VLA (8.4, 22, 43 GHz) and SCUBA sub-mm flux measurements for NGC 4649, NGC 4472, and NGC 4636 (joined by a solid line). NGC 4472 is the brightest source in the sample, its spectrum is quite steep and probably dominated by jet emission up to sub-mm wavelengths (see also the 43 GHz image, Fig. 1). The spectrum of NGC 4649 rises up to the 22 GHz but by 43 GHz the spectrum has turned over. SCUBA non-detection at 2000μ is represented as a 3σ upper limit. No SCUBA data are available for NGC 4636 but VLA measurements imply a flat spectrum with (possibly) a sharp cut off (3σ upper limit at 43 GHz). The synchrotron emission as predicted by the standard ADAF model (dashed-line; with typically $m = 10^9$, $\dot{m} = 1 \times 10^{-3}$, $\beta = 0.5$, $\alpha = 0.3$) greatly overestimates the total observed flux. The model is inconsistent with the radio limits for all three of the sources.

pointing and flux calibration. The SCUBA data were analysed using the dedicated SURF reduction package (Jenness 1998) using the techniques described by Ivison et al. (1998a, 1998b). The SCUBA flux measurements, are summarized in Table 2. Both VLA and SCUBA data are plotted in Fig. 2.

NGC 4649 – In accordance with the previous obser-

vations (Fabbiano et al. 1987; Wrobel et al. 1991) our VLA measurements imply that this source is strongly core dominated. Its spectrum, as measured by VLA and SCUBA shows evidence of a slowly rising, high frequency component up to ~ 30 GHz. The spectrum then sharply turns over, as implied by the 43 GHz measurement and the lack of a SCUBA detection (represented as 3σ upper limit) at 2000μ m.

NGC 4472 – The steeper spectral slope (Fig. 2) is probably due to the dominance of emission from a jet-like structure. Even at 43 GHz (Fig. 1) the emission is still fairly extended. The extended component probably dominates all the way into the SCUBA frequencies.

NGC 4636 – This galaxy showed the presence of a flat component in its spectrum in the 1.4 and 4.75 GHz measurements of Fabbiano et al. (1987). The relative contributions of the core components in this source is clearly illustrated in the maps of our 8 GHz and 22 GHz VLA observations, shown in Fig. 1. Our VLA high-frequency observations imply a relatively sharp turn over in the spectrum at around 10 GHz. At 43 GHz only a (3σ) upper limit could be set to the the source flux. Sub-millimetre observations of this object were not performed.

2.3 The X-ray data

Einstein Observatory observations of giant elliptical galaxies reveal that the overall X-ray emission is generally extended with most of it arising from the hot gas at $kT \sim 1$ keV (Fabbiano, Kim & Trinchieri, 1992).

Here we examine *ROSAT* HRI datasets in order to constrain the nuclear X-ray flux of NGC 4472 and NGC 4636 (see Di Matteo & Fabian, 1997 for the analysis of NGC 4649). Fig. 3 shows the HRI image of NGC 4472 and NGC 4636. Consistent with the *Einstein* HRI observations, the *ROSAT* HRI image shows that these sources are extended with most of the emission coming from hot gas in the interstellar medium. The low luminosity radio activity though, indicates that there is some form of active central engine in the core of these galaxies. In order to find an upper limit to their nuclear emission (i.e. a maximum possible luminosity of a point source) we fit the surface brightness profile with

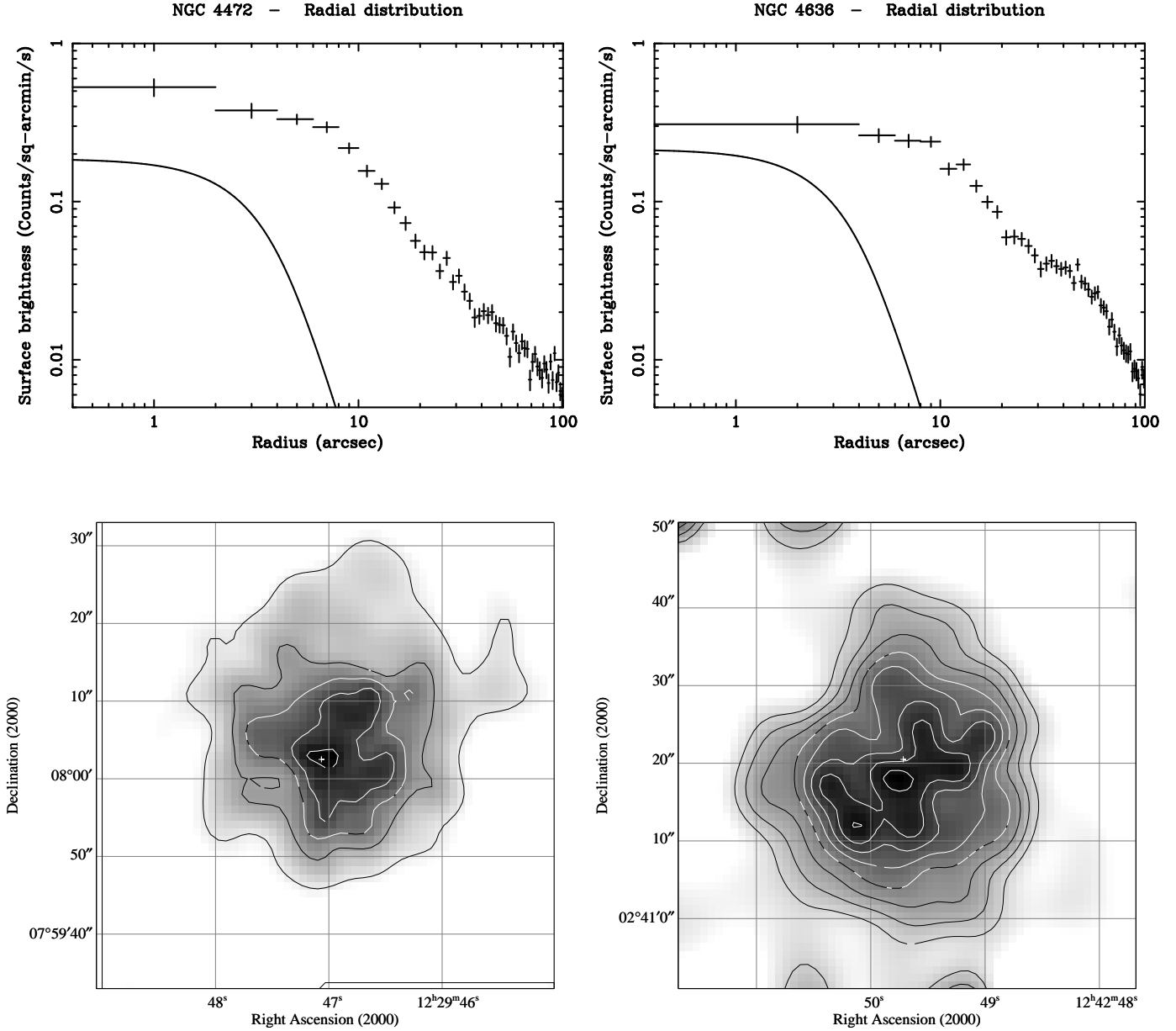


Figure 3. The core regions of NGC 4472 (on the right) and NGC 3636 (on the left) as imaged in 27 ks and 22 ks exposures respectively with the *ROSAT* HRI. The distribution of the X-ray emission of the central region of both galaxies is quite complex and asymmetric. The diffuse emission is from the hot interstellar medium. The images have been smoothed adaptively prior to contouring; the minimum number of counts over which smoothing occurred is 20. Contour levels are equally spaced on a logarithmic scale, starting at $3 \times 10^{-3} \text{ count s}^{-1} \text{ arcmin}^{-2}$ and increasing by a factor 1.6 between adjacent contours (NGC 4472) and starting at $8 \times 10^{-4} \text{ count s}^{-1} \text{ arcmin}^{-2}$ and increasing by a factor 1.3 (NGC 4636). On top, we also show the radial distribution of the surface brightness and the contribution of a point source to their emission. The solid line shows the PSF of the *ROSAT* HRI compared to the total count rate per unit area.

an extended component modelled by a King profile plus a point source modified by the Point Spread Function (PSF) of the HRI (see Fig. 3).

NGC 4472 – We analyse the *ROSAT* HRI data resulting from a 27 367 s exposure. Our formal 3σ upper limit, assuming no intrinsic absorption, predicts a count rate from the point source component of $2.1 \times 10^{-3} \text{ ct s}^{-1}$ (Fig. 3). Assuming the spectrum to be a power-law with a canonical photon index $\Gamma = 2.0$ modified by the effects of Galactic absorption (with column density $N_{\text{H}} = 3.0 \times 10^{20} \text{ cm}^{-2}$);

this count rate implies a flux density at 1 keV of $F(1 \text{ keV}) = 6.8 \times 10^{-14} \text{ erg cm}^{-2} \text{ s}^{-1} \text{ keV}^{-1}$. This result is fairly insensitive to the choice of power law index.

NGC 4636 – We analyze the joint *ROSAT* HRI data resulting from 13 264 s and 8 688 s exposures. The formal 3σ upper limit assuming no intrinsic absorption predicts a count rate from the point source component of $2.5 \times 10^{-3} \text{ ct s}^{-1}$ (Fig. 3). Assuming the same energy distribution described above this count rate corresponds to a flux density at 1 keV of $F(1 \text{ keV}) = 7.8 \times 10^{-14} \text{ erg cm}^{-2} \text{ s}^{-1} \text{ keV}^{-1}$.

NGC 4649 – see analogous analysis in Di Matteo & Fabian (1997).

3 ADAFS AROUND SUPERMASSIVE BLACK HOLES

In an advection-dominated accretion flow (ADAF) most of the energy released by viscous dissipation is stored within the gas and advected inward with the accreted plasma; only a small fraction is radiated away (see Narayan, Mahadevan & Quataret 1998 for a recent review). Work on ADAFs has been concerned with low- \dot{M} solutions (Rees 1982; Narayan & Yi 1995a,b; Abramowicz et al. 1995) which occur when the accretion rate is lower than a critical value, $\dot{m}_{\text{crit}} \lesssim 1.3\alpha^2$, (hereafter $\dot{m} = \dot{M}/\dot{M}_{\text{Edd}}$ in Eddington units). This optically-thin branch of the solutions makes use of the standard α viscosity and is based on certain critical assumptions. ADAF models assume that most of the viscous energy is deposited into the ions and only a small fraction of energy goes directly into the electrons. The energy is then transferred from the ions to the electrons via Coulomb collisions. Because Coulomb transfer in the low-density ADAF is inefficient, the plasma is two-temperature. The kinetic temperature of the ions reaches the virial temperature while the electron temperature saturates at around $10^9 - 10^{10}$ K.

The spectrum from an ADAF is very different from that of a standard thin disk. The high electron and ion temperatures, the presence of an equipartition magnetic field and the fact that the gas is optically thin, allow a variety of radiation processes to contribute to the emitted spectrum from radio to gamma rays. The radio to X-ray emission is produced by the electrons via synchrotron, bremsstrahlung and inverse Compton processes. The gamma-ray radiation results from the decay of neutral pions created in proton-proton collisions. Note that the radio emission from an ADAF is much stronger than that from a standard thin disk.

In the remainder of this section we summarize how we compute the spectrum of an ADAF based on the model of Narayan & Yi 1995 and recent calculations by Narayan, Barret & McClintock 1997 (hereafter NBM) and Esin, McClintock & Narayan 1998, (hereafter ESM).

3.1 The model

The modelling techniques have advanced significantly during the last two years (NBM, ESM). Here we briefly describe how the model of Di Matteo & Fabian (1997) has been improved by taking into account the advection of energy by electrons which, as pointed out by Nakamura et al. (1996) and Narayan, Barret & McClintock (1997), can be important. For convenience, we rescale the radial co-ordinate and define r by $r = R/R_S$, where R is the radial coordinate and R_S is the Schwarzschild radius of the hole.

In order to describe the dynamics we use the local self-similar solution calculated by Narayan & Yi (1995); this provides a reasonably accurate analytical estimate of the properties of the accretion flow. The dynamical model is uniquely specified by four structure parameters: α , the viscosity parameter, β , the ratio of magnetic to gas pressure, f , the advection parameter, which gives the ratio of advected energy to viscous heat input and γ , the adiabatic index of the

fluid which is assumed to be a mixture of gas and magnetic fields (Esin 1997); The models considered here are extremely advection-dominated so that f is virtually equal to 1 in all cases. For the present discussion the quantities of interest are:

$$\begin{aligned} v &= -2.1 \times 10^{10} \alpha c_1 r^{-1/2} \text{ cm s}^{-1}, \\ n_e &= 2.0 \times 10^{19} c_1^{-1} c_3^{-1} \alpha^{-1} m^{-1} \dot{m} r^{-3/2} \text{ cm}^{-3}, \\ B &= 6.6 \times 10^8 \alpha^{-1/2} (1 - \beta)^{1/2} m^{-1/2} \dot{m}^{1/2} r^{-5/4} c_1^{-1/2} c_3^{1/4} G, \\ \tau_{\text{es}} &= 12.4 \alpha^{-1} \dot{m} r^{-1/2} c_1^{-1}, \end{aligned} \quad (2)$$

where v is the radial velocity, n_e is the number density of electrons, B is the magnetic field strength, τ_{es} is the electron scattering optical depth, m is the black hole mass in solar units. c_1 and c_3 are the constants defined in Narayan & Yi 1995 and are functions of γ and f .

The thermodynamic state of the flow is described by the ion temperature $T_i \sim 10^{12} \beta r^{-1}$ K, which is to a very good approximation the virial temperature, the electron temperature T_e and the magnetic pressure, $p_{\text{mag}} = (1 - \beta)p_{\text{tot}}$. It is usually assumed that all of the structural parameters in the model are constant. In order to determine the spectral properties of the flow we need to calculate the electron temperature. The electron temperature profile is given by solving the electron energy balance equation (Nakamura et al. 1996, NBM, EMB)

$$\rho T_e v \frac{ds_e}{dR} = \rho v \frac{du_e}{dR} - k T_e v \frac{dn_e}{dR} = Q^{\text{ie}} + \delta Q^+ - Q^-, \quad (3)$$

where s_e is the entropy and the term on the left-hand side represents the rate at which energy in the electrons is advected inward in the flow (as shown by the two central terms, that is the rate of change of internal energy u_e and of compression heating/cooling). The other terms in equation Eqn. 3 are the rate at which electrons are heated by Coulomb collisions, Q^{ie} , the total rate of viscous dissipation, Q^+ (we assume $\delta \sim 10^{-3}$), and the radiative cooling Q^- . This latter term consists of electron-electron and ion-electron bremsstrahlung, synchrotron emission and its Comptonization (as in Di Matteo & Fabian 1997a). With the simple scaling laws in Eqn. 3 the above equation is a first order differential equation. We solve numerically the temperature balance equation with one outer boundary condition i.e. $Q^{\text{ie}} = Q^-$ at $r = r_{\text{out}} = 10^4$ (in the outer regions the flow collapses to one temperature and radiative cooling – dominated by bremsstrahlung in this regions – balances the Coulomb heating). Our approach for calculating the temperature profile is much simpler than the procedure described NBM, EMN but it is in fairly good agreement with their results.

Once the electron temperature profile has been determined (see e.g. Fig. 4) we calculate the radiation spectrum of an ADAF integrated over radius from $r_{\text{in}} \sim 3$ to $r_{\text{out}} \sim 10^3$. This includes: synchrotron, bremsstrahlung and Comptonization of the soft synchrotron photons. (Here the complicated problem of the global radiation energy transfer, see e.g. NBM, ENM, is not treated and local approximations are used). As we discuss later, the only tight constraints to the problem come from the radio data, where an ADAF radiates via synchrotron emission. In the thermal plasma of an ADAF, synchrotron emission rises steeply with decreasing frequency. Under most circumstances the emission

Table 4. Summary of data for the core of NGC 4649.

Frequency ν (Hz)	νF_ν (10^{-15} erg s $^{-1}$ cm $^{-2}$)	reference	notes
1.4×10^9	0.37	Hummel et al. (1983)	Westerbork
4.75×10^9	1.14	Fabbiano et al. (1987), Wrobel (1991)	Effelsberg, VLA
8.4×10^9	1.49	this work	VLA
1.07×10^{10}	2.78	Fabbiano et al. (1987)	Effelsberg
2.2×10^{10}	4.83	this work	VLA
3.3×10^{10}	10.5	Fabbiano et al. (1987)	Effelsberg
4.3×10^{10}	5.47	this work	VLA
1.5×10^{11}	≤ 7	this work	SCUBA
5.45×10^{14}	≤ 180	Byun et al. (1996)	HST
2.4×10^{17}	≤ 150	Paper 1	ROSAT HRI

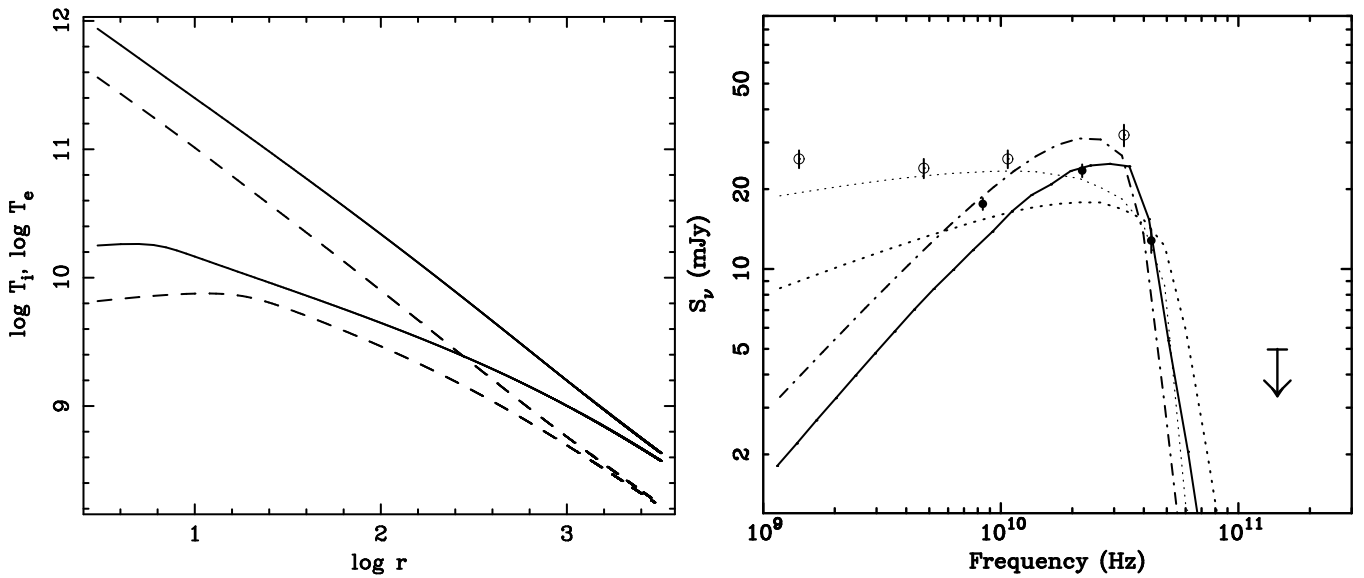


Figure 4. On the left, the temperature profile for an ADAF. The solid line is for $\beta \sim 0.99$ and the dashed line for $\beta = 0.5$. This corresponds to the mass and accretion rate of NCG 4649: for the other objects the temperature solution is very similar to the one shown. On the right, comparison between the synchrotron flux and the high energy radio and submillimeter limits for NGC 4649. The open circles represent the Fabbiano et al. (1987) measurements the filled circles and filled squares our VLA and SCUBA new limits. Our high energy measurements imply that the spectral turnover due to the self-absorbed synchrotron emission occurs at much lower frequencies than expected from previous a analysis (Di Matteo & Fabian 1997) and in general form the canonical ADAF model. The model is consistent with the data only if $\beta \lesssim 0.999$, i.e. a very low magnetic field (solid line), or if the emission is free-free absorbed by cold and dense material within $r_{\text{in}} = 17$. The dotted lines represent the case in which a magnetic wind carries away mass and angular momentum at large distances with $\dot{m} \propto (r/r_{\text{max}})^p$. The thicker dotted-line is for $r_{\text{max}} = 300$ and $p = 1$, the dashed line for $r_{\text{max}} = 200$ and $p = 1.2$.

becomes self-absorbed and gives rise to a black-body spectrum below a critical frequency ν_c . Above this frequency it decays exponentially as expected from a thermal plasma, due to the superposition of cyclotron harmonics. The synchrotron spectrum at each radius is calculated in the way described by Di Matteo, Celotti & Fabian (1997), following the optical-thin formalism developed by Mahadevan et al. (1996). With the relevant information about the original unscattered soft photon spectrum we can calculate the Compton scattered spectrum using the scattering kernel and redistribution functions derived by Poutanen (1994, and references therein). The bremsstrahlung spectrum in this semi-relativistic regime is best estimated with Stepney & Guilbert (1983) formalism. We also compute pion production by the

hot protons and the resulting γ -ray emission through pion decay (see Appendix A and also Mahadevan et al. 1997).

4 RESULTS

In this section we combine the modelling techniques outlined in the Section 3 and the data, with particular regards to the radio limits, from Section 2 to constrain the ADAF models in the context of elliptical galaxies.

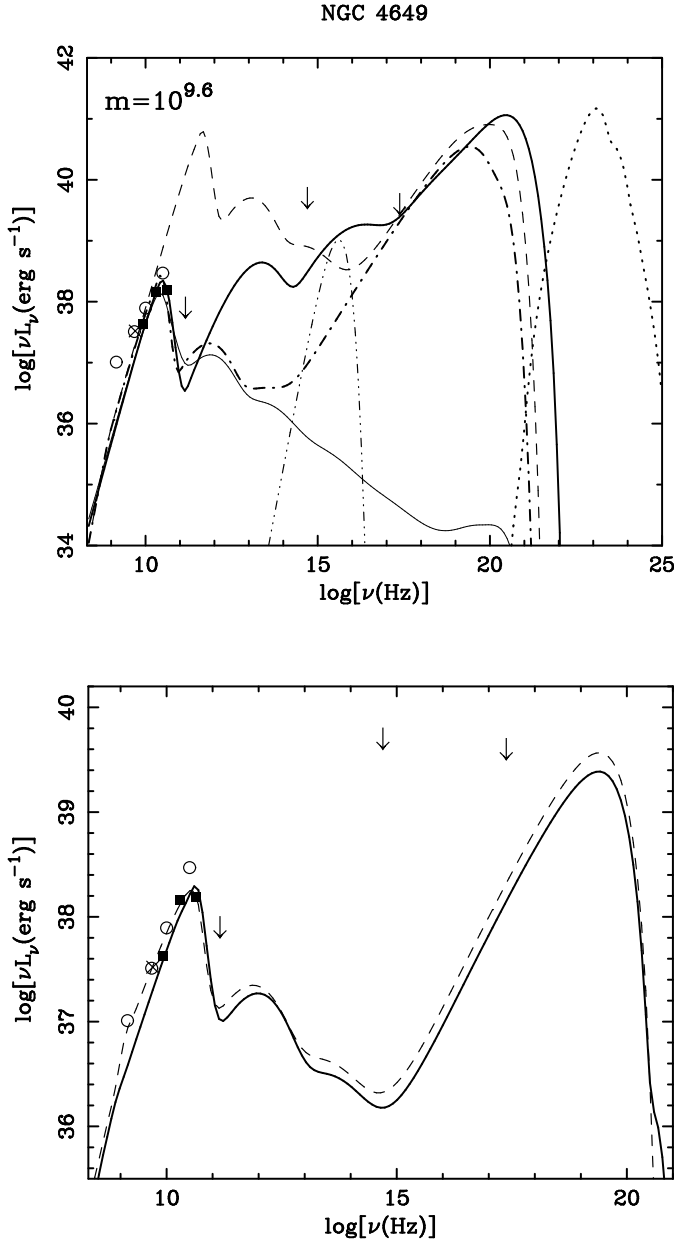


Figure 5. On top, the full band spectra calculated with an ADAF model. The same mass, $m = 10^{9.6}$, viscosity parameter, $\alpha = 0.3$ and respective Bondi rates are assumed for all of the different models (apart from (iv)). Four models are shown: (i) one for equipartition magnetic field, $\beta = 0.5$ –dashed line, clearly inconsistent with the radio limits (ii) one for $\beta = 0.999$ solid line, (iii) one for which the radio emission is free–free absorbed within $r_{\text{in}} = 17$, dashed–dot line and dash–dot–dot line (representative blackbody emission from the cold absorbing material), (iv) and one for which $\alpha = 0.3$, $\beta = 0.5$ and $\dot{m} \sim 10^{-6}$, thin solid line. At the bottom, the magnetic wind model with $\dot{m} \propto (r/r_{\text{max}})^p$. The solid line is for $r_{\text{max}} = 300$ and $p = 1$, the dashed line for $r_{\text{max}} = 200$ and $p = 1.2$. A distance of 15.8 Mpc is assumed. X-ray cooling processes dominate the emission.

4.1 The inconsistency between the radio data and the ‘canonical’ model predictions

Before presenting detailed models for the three sources and discussing each one of them separately, we would like to illustrate (more qualitatively) the apparent inconsistency between the ADAF predictions and our radio measurements. In Fig. 2 we show our VLA and SCUBA data points and the expected ADAF self–absorbed synchrotron emission (dashed line) from a super–massive black hole $m = 10^9$ accreting at $\dot{m} = 10^{-3}$ (typical order of magnitude black hole masses and Bondi rate in ellipticals). The canonical ADAF with $\alpha = 0.3$ and $\beta = 0.5$ is unequivocally ruled–out by our radio/sub–mm limits: it greatly overestimates the total possible contribution at these frequencies.

ADAF models have been applied to a number of accreting black holes systems: galactic black holes candidates, (e.g NBM, ENM) the centre of our galaxy (Sgr. A; Narayan et al. 1998) and low luminosity galactic nuclei (Lasota 1996, Reynolds et al. 1996, Di Matteo & Fabian 1997) All of those models seemed to be consistent with the choice of $\alpha = 0.3$ and $\beta = 0.5$ (exact equipartition). The canonical ADAF model (with such a choice of α and β) has been regarded as a one parameter model (e.g NBM); the only free parameter (adjusted to fit the X-ray data) being the mass accretion rate \dot{m} of the different systems. This cannot be applied to these low luminosity elliptical galaxy systems any longer. As we shall show in the course of this section, the severe discrepancy between the radio and sub–mm observations with the ADAF model predictions raises serious issues about the explanation for low–luminosity systems. Although the present VLA and SCUBA observations do not rule out the presence of an ADAF in these elliptical galaxies cores, they do place new (very tight) constraints on the physical properties of any proposed ADAF, the plausibility of which remains an object of discussion. Further studies might be necessary to fully address the different factors regulating low–luminosity systems.

For all three elliptical galaxies analyzed here we now have a black hole mass determination from Magorrian et al. (1998), shown in Table 1, and their respective accretion rates estimated from the Bondi rate in Eqn. 1. By invoking exact equipartition and $\alpha \sim 0.3$, as done in previous work, our systems are virtually parameter–free; but we are unable to obtain consistency with the radio data (see dashed lines in Fig. 5 and 6. Because of the apparent consistency with the (although looser) optical and X-ray limits we are prompted to hypothesise that either a lower magnetic field strength might be the cause of the lack of synchrotron emission or the emission is free–free absorbed by clumps of cold and dense matter. Also a magnetic wind or outflow might operate in these systems and remove most of the mass and angular momentum at large distances so that the central densities and emissivities are much smaller than in a standard ADAF. We will analyze mainly these three possibilities and keep m and \dot{m} (apart from Section 4.4) as set from above (the thin solid line in Fig. 5 shows a model for which $\beta \approx 0.5$, $\alpha \approx 0.3$, i.e. the ‘standard’ ADAF parameters, and where \dot{m} is varied as to fit the radio limits. We find that in order to be consistent with the radio measurements the accretion rate has to be very (implausibly) small, $\dot{m} \approx 10^{-6}$ i.e. $\dot{M} \sim 10^{-5} M_{\odot} \text{yr}^{-1}$).

Because of the jet-dominated emission in NCG 4472 and the lack of any high energy component in NGC 4636, we mainly concentrate our modelling on NGC 4649 which is strongly core dominated and whose spectrum shows indications of a sharp turnover. As shown in Fig. 5 and 6 the computed spectrum has five major peaks. From the left these correspond to self-absorbed thermal synchrotron emission, doubly-Comptonized synchrotron emission, bremsstrahlung emission and γ -rays from neutral pion decay.

4.2 High β ADAFs

The solid lines in Fig. 4, 5 and 6 demonstrate the comparison between an ADAF model, with very low magnetic field, and the data. As β is increased to $\lesssim 0.99$ ($B \propto (1 - \beta)^{1/2}$, see Eqn. (2)) the agreement with the radio limits improves significantly. The decrease in magnetic field strength with respect to the equipartition value is quite severe. This is required by the fact that the luminosity (approximated by the Rayleigh-Jeans limit) at the self-absorbed frequency peak $\nu_c (\propto BT_e^2)$ scales as

$$\nu_c L_{\nu c} \propto \alpha^{-3/2} (1 - \beta)^{3/2} T_e^7 m^{1/2} \dot{m}^{3/2}, \quad (4)$$

i.e. the power output is a very strong function of T_e , which increases as β increases. With the inclusion of advection for the electrons, the low \dot{m} , $\dot{m} \ll \dot{m}_{\text{crit}}$, flows are effectively adiabatic and the electron temperature is basically determined by the balance between the increase by adiabatic compression and the decrease by radiative cooling (Nakamura et al. 1997, NBM). As a result of this, for low magnetic fields ($\beta \lesssim 1$) the temperature increases almost monotonically (Fig. 4). For strong fields the rise of T_e is suppressed by very efficient synchrotron and Compton cooling and the temperature in the inner regions of the flow is almost constant (see Fig. 4).

The solid line in Fig. 5 shows the model for NGC 4649 in which B is ~ 1 per cent of the equipartition magnetic field. The model is consistent with the high energy VLA and SCUBA upper limit. It is fairly discrepant with the Fabbiano et al. lower frequency measurements where the contribution from a jet might become more relevant (Fig. 1). If all of the emission were to originate from (or be dominated by) a separate jet component, the particle energy distribution would need to be very sharply cut off in order for the emission practically to die out between 5×10^{10} Hz and $\sim 10^{11}$ Hz, as implied by our high energy VLA and SCUBA constraints (see also discussion at the end of Section 4.3). As mentioned before, the large spectral break can be naturally accounted for by thermal synchrotron radiation in ADAF models. A similar discussion could also apply to NGC 4636 (Fig. 6), where a relatively sharp spectral turnover seems to be occurring at $\sim 10^{10}$ Hz. (Although the lack of any higher energy measurements for this objects make the situation less clear). Also, an upper limit ADAF contribution to the much flatter, probably jet-originating, radio spectrum of NGC 4472 limits B to be within a few percent of the equipartition value.

Because the system is highly photon starved and $T_e \gtrsim 10^{10}$ K the Comptonized spectrum is extremely hard (see solid lines in Fig. 5 and Fig. 6) showing clearly the two Compton scattering orders. In this regime of $\dot{m} \sim 10^{-3}$,

bremsstrahlung emission usually dominates the X-ray emission and becomes increasingly important for higher black hole masses.

As shown in Eqn. (4) the peak luminosity is also inversely proportional to α . Higher values for the viscosity parameter would also decrease the luminosity and therefore allow for lower values of β (still implying a magnetic field strength B lower than equipartition).

Although such low magnetic energy densities, as invoked here, do not pose any real problem to the dynamics of an ADAF (which is supported by gas pressure) they appear quite implausible for astrophysical systems. Also, it is hard to reconcile the high viscosity parameter $\alpha \sim 0.3$ with the magnetic pressure becoming so small. According to recent studies (e.g. Balbus & Hawley 1996) α should be linearly correlated with the magnetic field in the disk (although it not clear at all how $\alpha \sim 0.3$ can be obtained from magnetic shear instabilities in an ADAF, which also saturates for magnetic fields in equipartition; the low magnetic field can still act as a catalyst for turbulence but could hardly be important enough to make α as high as it is required). The high viscosity could still be justified if global processes, such as a wind would operate to transport angular momentum away from the system.

4.3 Free-free absorption of synchrotron radiation by cold material

A small amount of very dense matter in the central region of an ADAF have an important effect on the emitted spectrum (Celotti, Fabian & Rees 1992). In particular, if a small fraction of the total amount of matter is in the form of small dense clouds much of the primary synchrotron radiation emitted by an ADAF would be absorbed. As examined by Ferland & Rees (1988) the radiative equilibrium of very dense gas irradiated by an intense source is dominated by free-free absorption which is extremely effective at depleting the low frequency radiation from the primary source (in this case the ADAF). The absorbed primary radiation is re-emitted as quasi-blackbody radiation at the equilibrium temperature. In other words, the magnetic field in an ADAF could be as high as in equipartition but the synchrotron emission suppressed. As discussed by Rees (1987) the relatively strong magnetic field in the flow, responsible for the production of the synchrotron radiation, can also provide the means of cloud confinement. The theoretically simplest possibility is that the gas is confined to small regions from which the magnetic field is excluded. The condition of pressure equilibrium (i.e. cloud thermal pressure balancing the compressive magnetic stresses) then imposes a maximum density $n_c \sim 10^{15} T_4^{-1} B_2^2 \text{ cm}^{-3}$ where a reference value of $T_4 \lesssim 10^4$ K has been assumed for the temperature of the gas in the clouds and $B_2 = 10^2 B_2 \text{ G}$ is the magnetic field in the vicinity of the hole from Eqn. (2) with $\beta \sim 0.5$ and $\alpha = 0.3$, $B_2 = 2(r/3)^{-5/4} (\dot{m}/10^{-3})^{1/2} (m/10^9)^{1/2}$ (see also Celotti & Rees 1998 for more details). With such density and temperature and absorption extending up to frequency $10^{12} \nu_{12}$ Hz the thickness of the absorbing region can be as small as $h \sim 30 T_4^{1/2} n_c^{-2} \nu_{12}^3 (1 - e^{-5 \times 10^{-3} \nu_{12}/T_4}) \text{ cm}$. A small volume filling factor can still be consistent with a large cov-

Table 5. Summary of data for the core of NGC 4472.

Frequency ν (Hz)	νF_ν (10^{-15} erg s $^{-1}$ cm $^{-2}$)	reference	notes
1.5×10^9	3.36	Wrobel (1991)	VLA
2.3×10^9	3.50	Wrobel (1991)	VLA
5.0×10^9	4.76	Wrobel (1991)	VLA
8.4×10^9	3.70	this work	VLA
2.2×10^{10}	6.82	this work	VLA
4.3×10^{10}	8.90	this work	VLA
1.5×10^{11}	14.0	this work	SCUBA
2.2×10^{11}	9.9	this work	SCUBA
3.5×10^{11}	10.5	this work	SCUBA
5.45×10^{14}	≤ 180	Byun et al. (1996)	HST
2.4×10^{17}	≤ 68	this work	<i>ROSAT</i> HRI

Table 6. Summary of data for the core of NGC 4636.

Frequency ν (Hz)	νF_ν (10^{-15} erg s $^{-1}$ cm $^{-2}$)	reference	notes
1.5×10^9	0.88	Wrobel (1991)	VLA
2.3×10^9	1.74	Wrobel (1991)	VLA
4.75×10^9	1.23	Fabbiano et al. (1987), Wrobel (1991)	Effelsberg, VLA
8.4×10^9	0.70	this work	VLA
1.07×10^{10}	2.57	Fabbiano et al. (1987)	Effelsberg
2.2×10^{10}	1.23	this work	VLA
4.3×10^{10}	≤ 0.77	this work	VLA
5.45×10^{14}	≤ 68.7	Byun et al. (1996)	HST
2.4×10^{17}	≤ 78.1	this work	<i>ROSAT</i> HRI

ering fraction if the clouds are very numerous, or if their thickness is much smaller than their length, i.e. filaments.

In our ADAF model, the synchrotron radiation at different frequencies is produced at different radii in the flow, the emission at $\sim 10^{12}$ Hz (see dashed lines in Fig. 5 and Fig. 6) coming from close to the black hole and the emission from lower frequencies coming from further out. It is plausible that the free-free absorption can be large enough to deplete most of the high energy emission within a certain radius. (If the clouds are sheared as they are accreted inward, their column density could go down. But because n_c increases in the higher pressure regions free-free opacity would still go up so that small- r absorption can be even more dominant).

The dash-dotted lines in Fig. 5 and 6 show a simple representation of such a model where $\beta = 0.5$, $\alpha = 0.3$, i.e. the 'canonical' ADAF values, and where the inner radius at which $f_c \sim 1$ has been constrained from the VLA and SCUBA measurements to be between $r_{\text{in}} \sim 15$ to 30 depending on the particular source. Fig. 5 also shows representative blackbody emission originating from the cold gas in the clouds (the detailed spectrum of the reprocessed and cloud emission is beyond the scope of this paper; it has been calculated in more detail by Kuncic, Celotti & Rees 1997).

Alternatively, within the context of this hypothesis, most of the emission could be free-free absorbed by cold

material in the disk and what we observe is only the radio emission from the small jets present in these objects. In this connection, we note that Falcke (1996; also Becker & Duschl 1997) has proposed non-thermal models for the radio emission in Sgr. A* assuming that most of the electrons have Lorentz factors of around a few hundred. By requiring that the nonthermal electrons have monoenergetic electron distribution, such a model would be able to reproduce the sharp cut-offs implied by our VLA and SCUBA observations of NGC 4649 and NGC 4636 (the nonthermal synchrotron usually has a spectral form $L_\nu \sim \nu^{-0.7}$; this means that the optically thin emission would otherwise continue to rise).

We note that any mechanism which removes (or hides) the inner part of the ADAF emission will suffice to bring the model into agreement. An ADAF down to $r \sim r_{\text{in}}$ and a Bondi flow down to the smallest radii. Time-variability is also a possibility, but it needs to be very extreme. This might be related to the large-scale random motions associated with dissipation in ADAFs (Blackman 1998) and (fairly implausibly) would need to affect the three objects systematically in the same direction. More promisingly, as we shall discuss below, a magnetic wind and/or an outflow could suppress the emission from the inner regions of the flow.

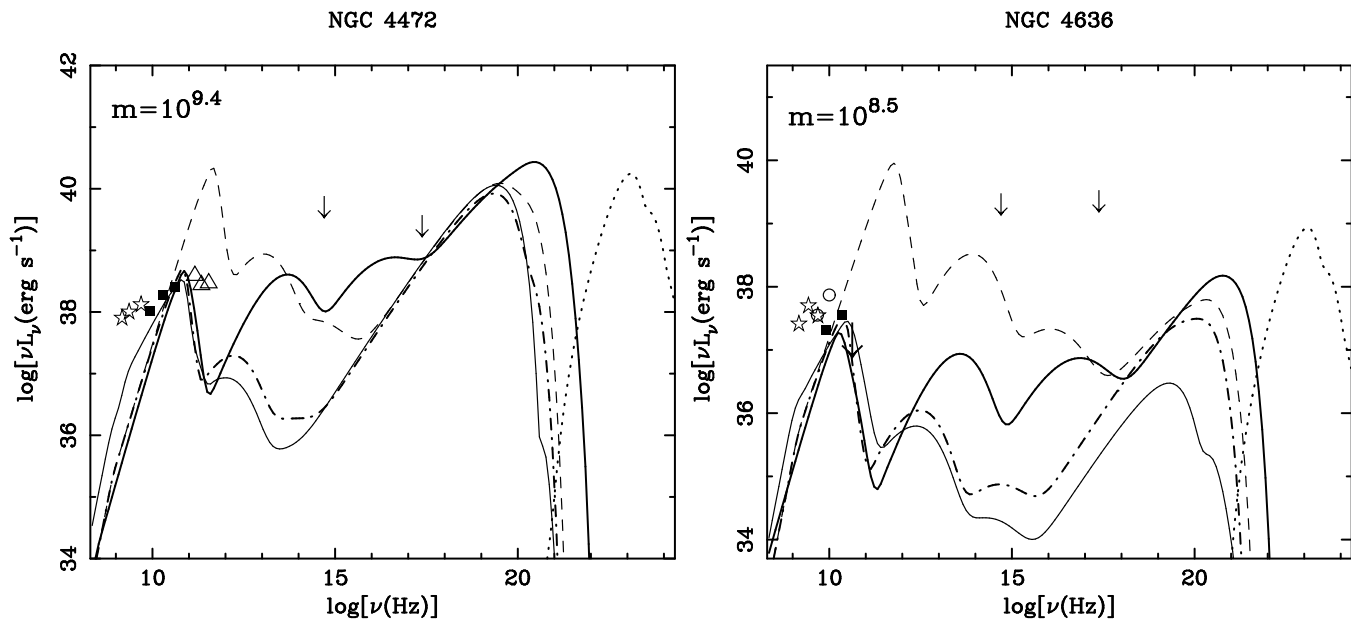


Figure 6. The full band spectra calculated with an ADAF model for NGC 4472 (on the left) and NGC 4636 (on the right). Black hole masses, given in Table 1, with the respective Bondi rates and the viscosity parameter, $\alpha = 0.3$, have not been changed in the different models. Four models are shown: (i) one for equipartition magnetic field, $\beta = 0.5$, dashed line, clearly inconsistent with the radio limits (ii) one for $\beta = 0.999$ (NGC 4636) and $\beta = 0.99$ for NGC 4472, solid line, (iii) one for which the radio emission is free-free absorbed within $r_{\text{in}} = 30$ (NGC 4636) and $r_{\text{in}} = 10$ for NGC 4472, dashed-dot line. Also (iv) the magnetic wind model with $\dot{m} \propto (r/r_{\text{max}})^p$. The thin solid lines are for $r_{\text{max}} = 90$ and $p = 1.2$ (NGC 4472), and for $r_{\text{max}} = 350$ and $p = 0.9$ (NGC 4636). Distances of 15.8 Mpc and 16 Mpc are assumed for NGC 4472 and NGC 4636 respectively. X-ray cooling processes dominate the emission.

4.4 Magnetic wind / outflow

It has been shown (Blandford & Payne 1982) that energy, angular momentum and mass can be removed magnetically from accretion disks, by field lines that leave the disk and extend to large distances. Within the context of a self-similar solution it is possible for such a magnetically driven wind to carry away most of the mass and angular momentum at large distances so that the central densities pressures and emissivities can be smaller than that of a standard ADAF (Begelman & Blandford in preparation); the flow can then be geometrically thinner than the standard ADAF. We find (Fig. 5, 6) that by taking $\dot{m} \propto r^p$ with $p \sim 1$ most of the emission from the inner regions of the flow is suppressed and the model is brought into agreement with the observations. The presence of a magnetically driven wind or some kind of an outflow not only seems plausible in this context, but may also be necessary in order for the ADAF solution to have a Bernoulli constant less than zero. As remarked by Narayan & Yi (1995) in the self-similar ADAF solution the Bernoulli parameter (defined as the sum of the kinetic energy, the potential energy and the enthalpy of the accreting gas) is positive implying that gas on any streamline can spontaneously escape to infinity. (In contrast to the standard thin disk, in the ADAF case radiation is suppressed and the excess energy production is stored as internal energy, making the Bernoulli constant positive).

If most of the mass (not just the angular momentum) can be extracted at large distances by magnetic torques, the fraction of mass that flows into the very central regions can be quite small. In Fig. 5 and 6 we show how the radio data can be explained by such a flow (a hydromagnetic

wind can potentially be totally non-radiating; Blandford & Payne 1982) when we adopt a simple model in which the accretion rate decreases as r decreases. We take $\dot{m} = \dot{m}_{\text{Bondi}}$ down to a maximum radius r_{max} and $\dot{m} = \dot{m}_{\text{Bondi}}(r/r_{\text{max}})^p$ from r_{max} all the way into the centre, where typical values of p and r_{max} are ~ 1 and \sim a few 100, respectively. Figs. 5 and 6 illustrate how a decreasing \dot{m} greatly affects the high frequency synchrotron emission component (and its Comptonization) and not so drastically the bremsstrahlung (as much of its contribution comes from outer parts of the flow). Note, though, that UV/X-ray measurements would be able to discriminate between this model from those in the previous Sections (4.2 and 4.3). Also, because of the additional dependence of \dot{m} on r the slope of the self-absorbed synchrotron radiation flattens as p increases. In the case of NGC 4649 therefore the slope of the observed spectrum sets an upper limit to p which cannot much exceed ~ 1 (see Fig. 4) so that $r_{\text{max}} \sim 300$. Finally, because at large distances from the disc, the inertia of the gas can cause the magnetic field to become increasing toroidal, the magnetic stresses could be responsible for converting the centrifugal outflow into a more collimated jet structure (observed in the radio, see Fig. 1. The flow might be more similar to an ion-supported torus (Rees et al. 1982) which includes outflows in funnels. If an outflow does occur (as seems to be the case for NGC 4472 and NGC 4636) it must be fairly well collimated in order that it does not invalidate our accretion estimates. It is possible that an outflow makes the accretion rate unsteady.

5 SUMMARY & DISCUSSION

Previous work (Fabian & Rees 1995, Reynolds et. al. 1996, Di Matteo & Fabian 1997, Mahadevan 1997) has suggested that accretion of hot gas in an elliptical galaxy may create the ideal circumstances for an ADAF to operate. The present observational studies, aimed at finding further evidence for of such accretion mode, have shown that new strong physical constraints need to be introduced to the proposed central ADAF in such systems. We have examined new high frequency VLA and sub-mm SCUBA observations of the three giant, low-luminosity elliptical galaxies NGC 4649, NGC 4472 and NGC 4636. At these frequencies the ADAF model predicts that the emission is dominated by self-absorbed thermal synchrotron radiation. Our new radio limits show a severe discrepancy with the canonical ADAF predictions and significantly overestimate the observed flux. While the present observations do not rule out the presence of an ADAF in the systems considered, they do place strong constraints on the model. We have discussed how the emission could be suppressed because either (1) the magnetic field in the flow is extremely low (if the viscosity parameter α can still be high enough) or (2) synchrotron emission is free-free absorbed by cold material in the accretion flow. Finally, (3) we discuss how slow non-radiating accretion flows may drive winds to remove energy, angular momentum and mass so that the central densities, pressure and emissivities are much smaller than in a standard ADAF. As most of the accreting gas is lost at large distances, this scenario becomes particularly appealing for explaining very low luminosity systems. The present observations raise serious issues about the explanation for the quiescence of elliptical galaxies nuclei and possibly other nearby systems now known to possess quiescent supermassive black holes.

The validity of our findings is strengthened by recent radio observations of another source, NGC 4258 (Herrnstein et al. 1998), whose accretion is also modelled via an ADAF (Lasota et al. 1996). The case of NGC 4258 is particularly illustrative: because the relative position of the centre of mass of the sub-parsec molecular disk can be measured to a fraction of a milliarcsecond with VLBI, NGC 4258 has provided a rare opportunity to circumvent the ambiguity associated with core-jet emission and to test the radio predictions of the ADAF spectrum directly. The potential synchrotron emission in that case also overestimates the maximum possible contribution allowed by the 22 GHz upper limit of Herrnstein et al. The authors show that the potential ADAF must occur within $r = 10^2$. Our two proposed possibilities for the suppression of synchrotron emission would still be viable for NGC 4258. In particular, the shearing in the accretion disk might lead to the disruption of cold dense clouds as the material is accreted inward. The covering fraction might in this case be high enough even in the outer regions, to suppress the lower energy synchrotron radiation. Clearly in the case of NGC 4258 higher frequency radio measurements (probing the small- r emission and a possible spectral turnover) could easily test the plausibility of such an hypothesis.

In conclusion, the compelling observational evidence for ADAFs in low-luminosity systems, which could have potentially been found through high radio frequency and sub-mm observations, is still missing. Theoretically, the existence of advection-dominated solution is based on certain critical as-

sumptions, the plausibility of which still needs to be assessed fully. Although ADAFs have been promisingly applied to a great variety of low-luminosity systems, and convincingly to our galactic centre (Mahadevan 1998, NBM), questions concerning their universality must necessarily be addressed. Recent development of ADAF models represents an important step towards the understanding of low efficiency accretion, but further studies are necessary to fully address the different factors regulating low-luminosity systems. X-ray *AXAF* studies would be crucial for potentially resolving the faint point sources in the nuclei of these elliptical galaxies and therefore providing clues for understanding the fuelling of nearby massive black holes and for potentially discriminating between the different physical constraints on ADAFs we have discussed in the course of this study.

ACKNOWLEDGEMENTS

We are very grateful to Juri Poutanen for providing us a code to calculate inverse Compton spectra and to Steve Allen for carrying out the deprojection analysis. We thank Ramesh Narayan, Eric Blackman and Rohan Mahadevan for discussions. TDM acknowledges PPARC and Trinity College, Cambridge, for support. ACF thanks the Royal Society for support. RJI is supported by a PPARC Advanced Fellowship. The ASTERIX software package has been used for the X-ray data analysis. The National Radio Astronomy (NRAO) is a facility of the National Science Foundation, operated under cooperative agreement by Associated Universities, Inc.

REFERENCES

- Abramowicz M., Chen X., Kato S., Lasota J. P., Regev O., 1995, *ApJ*, 438, L37
- Blackman E.G., 1998, *MNRAS*, submitted
- Blandford R.D., Payne D.G., 1982, *MNRAS*, 199, 883
- Bondi H., 1952, *MNRAS*, 112, 195
- Byun Y., et al. 1996, *AJ*, 111, 1889
- Celotti A., Fabian A.C., Rees M.J., 1992, *MNRAS*, 255, 419
- Celotti A., Rees M.J., 1998, submitted
- Dermer C., 1986a, *ApJ*, 307, 47
- Dermer C., 1986b, *A&A*, 157,223
- Di Matteo T. 1998, PhD thesis, in preparation
- Di Matteo T., Celotti A., Fabian A.C., 1997, 291, 805
- Di Matteo T., Fabian A.C., 1997, *MNRAS*, 286, L50
- Di Matteo T., Fabian A.C., 1997a, *MNRAS*, 286, 393
- Esin A.A., McClintock J.E., Narayan R., 1997, *ApJ*, 489, 865
- Fabian A. C., Canizares C. R., 1988, *Nat*, 333, 829
- Fabian A. C., Rees M. J., 1995, *MNRAS*, 277, L55
- Fabbiano G., Kim D.W., Trinchieri G., *ApJS*, 1992, 80, 531
- Fabbiano G., Klein U., Trinchieri G., Wielebinski R., 1987, *ApJ*, 312, 111
- Falcke H., 1996, in *IAU Symp.* 169, Unsolved problems of the Milky way, ed. L. Blitz & P.J. Teuben (Dordrecht: Kluwer), 163
- Ferland G.J., Rees M.J., 1988, *ApJ*, 332, 141
- Ford H. C. et al. 1995, *ApJ*, 1994, 435, L27
- Harms R. J. et al., 1994, *ApJ*, 435, L35
- Herrnstein J.R., Greenhill L.J., Moran J.M., Diamond P.J., Inoue M., Nakai N., Miyoshi M., 1998, *ApJ*, submitted
- Ivison R.J., Dunlop J.S., Hughes D.H., Archibald E.N., Stevens

- J.A., Holland W.S., Robson E.I., Eales S.A., Rawlings S., Dey A., Gear W.K., 1998a, *ApJ*, 494, 211
- Iverson R.J., Smail I., Le Borgne J.-F., Blain A.W., Kneib J.-P., Bezecourt J., Kerr T.H., Davies J.K., 1998, *MNRAS*, , 298, 583 (astro-ph/9712161)
- Holland W.S., Gear W.K., Lightfoot J.F., Jenness T., Robson E.I., Cunningham C.R., Laidlaw K., 1998, in Phillips T.G., ed, *Advanced Technology MMW, Radio, and Terahertz Telescopes*, Proc. of SPIE Vol. 3357, in press
- Hummel E., Kotani C. G., Ekers R. D., 1983, *A&A*, 127, 205
- Kormendy J., Richstone D. 1995, *ARA&A*, 33, 581
- Kuncic Z., Celotti A., Rees M.J., 1997, *MNRAS*, 717
- Macchetto, F., Marconi A., Axon D.J., Capetti A., Sparks W., Crane P., 1997, *ApJ*, 489, 579
- Magorrian J. et al., 1998, *AJ*, 115, 2285
- Mahadevan R., 1997, *ApJ*, 477, 585
- Mahadevan R., 1998, *Nature*, in press
- Mahadevan R., Narayan R., Yi I., 1996, *ApJ*, 465, 327
- Mahadevan R., Narayan R., Krolick J., 1997, *ApJ*, 486, 268
- Narayan R., Barret D., McClintock J., 1997, *ApJ*, 482, 448
- Narayan R., Yi I., 1995a, *ApJ*, 444, 231
- Narayan R., Mahadevan R., Quataert E., 1998, to appear in "The Theory of Black Hole Accretion Discs", eds. M. A.Abramowicz, G. Bjornsson, and J. E. Pringle, (Cambridge University Press)
- Poutanen, 1994, PhD thesis, University of Helsinki
- Poutanen J., Svensson, R. 1996, *ApJ*, 470, 710
- Rees M. J., 1982, in Riegler G., Blandford R., eds, *The Galactic Center*. Am. Inst. Phys., New York, 166
- Rees M.J., 1987, *MNRAS*, 228, 47p
- Rees M. J., Begelman M. C., Blandford R. D., Phinney E. S., 1982, *NAT.*, 295, 17
- Reynolds C. S., Di Matteo T., Fabian A. C., Hwang U., Canizares C. R., 1997, *MNRAS*, 283, L111
- Robson E.I., Holland W.S., Gear W.K., Lightfoot J.F., Jenness T., Iverson R.J., Stevens J.A., Sandell G., Cunningham C.R., Ade P.A.R., Griffin M.J., Duncan W.D., Murphy A.S., Naylor D.A., 1998, *MNRAS*, submitted
- Sadler E. M., Jenkins C. R., Kotanji C. G., 1989, *MNRAS*, 240, 591
- Slee O. B., Sadler E. M., Reynolds J. E., Ekers R. D., 1994, *MNRAS*, 269, 928
- Stanger V. J., Warwick R. S., 1986, *MNRAS*, 220, 363
- Stecker F.W., 1971, *Cosmic Gamma Rays* (NASA SP-249), Washington D.C.
- Stephens S. A., Badhwar G.D., 1981, *Astrophysics and Space Science*, 76, 213
- Stepney S., Guilbert P. W., 1983, *MNRAS*, 204, 1269
- Tremaine S, 1995, *AJ*, 110, 628
- Wrobel J. M., 1991, *AJ*, 101, 127
- Wrobel J. M., Heeshen D.S., 1991, *AJ*, 101, 148

APPENDIX A: GAMMA-RAY EMISSION FROM ADAFS

The production of γ -rays from proton proton collisions is a two step process and has been calculated in detail by Stecker (1971, and also Stephens & Badhwar 1981; Dermer 1986ab). The colliding protons produce a neutral pion π^0 , which then decays into two γ -rays. Within the context of ADAF models pion emission can become relevant and it has been calculated by Mahadevan et al. (1997). Here, we consider a power law distribution of proton energy described by a spectral index p (as expected if energy is viscous energy is dissipated directly into the protons; for pion production

for a thermal distribution see Di Matteo 1998). The pion spectrum is then given by:

$$F(E_\pi) = \frac{I(p, \alpha, \beta)m\dot{m}}{m_\pi} \int_1^\infty \gamma^{-p} (1 - \gamma)^{-1/2} \frac{d\sigma_{\text{mb}}(\gamma_\pi, \gamma)}{d\gamma_\pi} d\gamma \quad (\text{A1})$$

photons $\text{s}^{-1} \text{GeV}^{-1}$

where $I(p, \alpha, \beta)m\dot{m}$ is given in Mahadevan et al. 1997 and it includes the integral over radius of the energy distribution function and the density of protons. γ is the Lorentz factor, $m_\pi = 0.135 \text{GeV}/c^2$ and $d\sigma_{\text{mb}}(\gamma_\pi, \gamma)/d\gamma_\pi$ is the differential cross-section determined by the isobar model (Stecker 1971) and the scaling model (Stephens and Badhwar 1981) used in the respective ranges.

To obtain the γ -ray emission, we calculate the integrals above and use the relation (Stecker 1971),

$$F(E_\gamma) = 2 \int_{E_{\pi\text{min}}}^\infty \frac{F(E_\pi)}{\sqrt{E_\pi^2 - m_\pi^2}}, \quad (\text{A2})$$

in photons $\text{s}^{-1} \text{GeV}^{-1}$, and where $E_{\pi\text{min}}$ is the minimum pion energy required to produce a γ -ray with energy E_γ ,

$$E_{\pi\text{min}} = E_\gamma + \frac{m_\pi^2}{4E_\gamma^2}. \quad (\text{A3})$$